

Site-Directed Alkylation of $[\text{EFe}_3(\text{CO})_9]^{2-}$ (E = S, Se, Te) Mediated by the Chalcogenide. Synthesis, Spectroscopic Characterization, and Reactivity of $[\text{PPN}][\text{MeFe}_3(\text{CO})_9\text{E}]$ (E = Se, Te)

Jaap Willem van Hal and Kenton H. Whitmire*

Department of Chemistry, MS 60, Rice University, 6100 Main Street, Houston, Texas 77005-1892

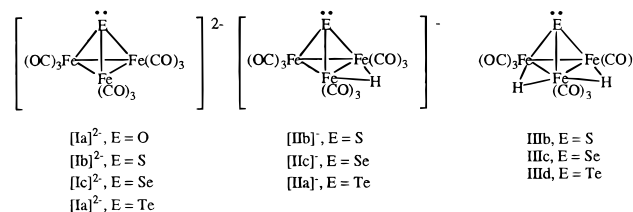
Received May 26, 1998

The compounds $[\text{PPN}]_2[\text{EFe}_3(\text{CO})_9]$ (E = S ($[\text{PPN}]_2[\text{Ib}]$), E = Se ($[\text{PPN}]_2[\text{Ic}]$), and E = Te ($[\text{PPN}]_2[\text{Id}]$)) ($\text{PPN} = [(\text{Ph}_3\text{P})_2\text{N}]^+$) were alkylated using methyl triflate or methyl iodide. $[\text{PPN}]_2[\text{Ib}]$ reacted with methyl triflate at the sulfur atom to form $[\text{PPN}][\text{Fe}_3(\text{CO})_9\text{SMe}]$ ($[\text{PPN}][\text{IVb}]$). In contrast, alkylation of $[\text{PPN}]_2[\text{Ic}]$ and $[\text{PPN}]_2[\text{Id}]$ occurred at the metal framework giving $[\text{PPN}][\text{MeFe}_3(\text{CO})_9\text{E}]$ (E = Se, $[\text{PPN}][\text{Vc}]$, Te = $[\text{PPN}][\text{Vd}]$), of which $[\text{PPN}][\text{Vc}]$ was characterized by X-ray crystallography. Compounds $[\text{PPN}][\text{Vc}]$ and $[\text{PPN}][\text{Vd}]$ represent new examples of the uncommon class of cluster compounds having alkyl groups terminally bound to a metal carbonyl cluster compound. The crystal structure of $[\text{PPN}][\text{Vc}]$ shows a long Fe–Me distance of 2.226(9) Å. The removal of electron density from the parent clusters $[\text{Ic}]^{2-}$ and $[\text{Id}]^{2-}$ could be seen in the trends of the ^{77}Se or ^{125}Te chemical shifts for $[\text{Vc}]^-$, $[\text{Vd}]^-$, and some structurally related compounds.

Introduction

The incorporation of a main group metal into the transition metal cluster framework has a profound influence on the stability, binding, and reactivity of the compound.^{1–6} For instance, $[\text{Fe}_3(\text{CO})_{11}]^{2-}$ reacts readily with CO to form $\text{Fe}(\text{CO})_5$, but $[\text{SeFe}_3(\text{CO})_9]^{2-}$ remains unchanged even after prolonged exposure to high pressures of CO and high temperatures.⁷ This makes the latter class of compounds potentially useful for catalytic cycles involving CO. Previous work using superheated MeOH for the synthesis of chalcogen–iron carbonylates indicated that the MeOH solvent could alkylate the chalcogen atom,⁸ as evidenced by the structural characterization of the $[\text{M}_4(\text{Te}_2)_2(\text{TeMe})_2(\text{CO})_8]^{2-}$ (M = Ru, Fe) prepared under those conditions. On the other hand, reactivity studies using Lewis and protic acids^{9–15} as well as Fenske Hall calculations¹⁶ showed that the

main nucleophilicity of the $[\text{EFe}_3(\text{CO})_9]^{2-}$ ($[\text{Ia}]^{2-}$, E = O; $[\text{Ib}]^{2-}$, E = S; $[\text{Ic}]^{2-}$, E = Se; $[\text{Id}]^{2-}$, E = Te) lies in the Fe_3 base (II^- and III). This makes this series of compounds an excellent choice for probing the site specificity of various electrophiles as a function of E.



In contrast to the many postulated catalytic processes involving alkyl groups bound to metal aggregates and surfaces, well-characterized examples of metal carbonyl clusters containing terminal alkyl groups remain uncommon. Examples include $[\text{Os}_3(\text{CO})_{10}(\mu\text{-Me})(\text{H})]$ (which exists as the methylene-bridged tautomer $[\text{Os}_3(\mu\text{-CH}_2)(\mu\text{-H})_2(\text{CO})_{10}]$),¹⁷ $\text{HOS}_2(\text{CO})_8\text{Me}$,¹⁸ $\text{Os}_2(\text{CO})_8\text{Me}_2$,¹⁹ $(\text{CO})_5\text{-MnRe}(\text{CO})_2(\text{PrNCHC}_5\text{H}_5\text{N})$,²⁰ $(p\text{-tolylNH})_2\text{Ir}_2(\text{CO})_4(\text{I})$,²¹ $(\text{OC})_5\text{ReOs}(\text{CO})_4\text{CH}_3$,²² $[\text{Fe}_2(\mu\text{-Me})(\mu\text{-CO})(\mu\text{-dppm})(\text{Cp})_2]$

* To whom all correspondence should be addressed.

- (1) Shriver, D. F.; Kaesz, H. D.; Adams, R. D. *The Chemistry of Metal Cluster Complexes*; VCH Publishers: New York, 1990.
- (2) Dimaio, A.-J.; Rheingold, A. L. *Chem. Rev.* **1990**, *90*, 169.
- (3) Whitmire, K. H. *J. Cluster Sci.* **1991**, *2*, 231.
- (4) Whitmire, K. H. *Adv. Organomet. Chem.*, in press.
- (5) Roof, L. C.; Kolis, J. W. *Chem. Rev.* **1993**, *93*, 1037.
- (6) Kanatzidis, M. G.; Huang, S.-P. *Coord. Chem. Rev.* **1994**, *130*, 509.
- (7) Bachman, R. E.; Whitmire, K. H. *Inorg. Chem.* **1994**, *33*, 2527.
- (8) Das, B.; Kanatzidis, M. G. *Inorg. Chem.* **1995**, *34*, 1011.
- (9) Roof, L. C.; Smith, D. M.; Drake, G. W.; Pennington, W. T.; Kolis, J. W. *Inorg. Chem.* **1995**, *24*, 337.
- (10) Shieh, M.; Tsai, Y.-C. *Inorg. Chem.* **1994**, *33*, 303.
- (11) Fischer, K.; Deck, W.; Schwarz, M.; Vahrenkamp, H. *Chem. Ber.* **1985**, *118*, 4946.
- (12) Roland, E.; Fischer, K.; Vahrenkamp, H. *Angew. Chem., Int. Ed. Engl.* **1983**, *22*, 326.
- (13) Marko, L.; Takacs, J.; Papp, S.; Marko-Monostov, B. *Inorg. Chim. Acta* **1980**, *45*, L189.
- (14) Marko, L. *J. Organomet. Chem.* **1982**, *213*, 271.
- (15) Bachman, R. E.; Whitmire, K. H.; van Hal, J. *Organometallics* **1995**, *14*, 1792.

(16) Schauer, C. K.; Harris, S.; Sabat, M.; Voss, E. J.; Shriver, D. F. *Inorg. Chem.* **1995**, *34*, 5017.

(17) (a) Calvert, R. B.; Shapley, J. R. *J. Am. Chem. Soc.* **1978**, *100*, 7726. (b) Schultz, A. J.; Williams, J. M.; Calvert, R. B.; Shapley, J. R.; Stucky, G. D. *Inorg. Chem.* **1978**, *18*, 319.

(18) Carter, W. J.; Kelland, J. W.; Okrasinski, S. J.; Warner, K. E.; Norton, J. R. *Inorg. Chem.* **1982**, *21*, 3955.

(19) Motyl, K. M.; Norton, J. R.; Schauer, C. K.; Anderson, O. P. *J. Am. Chem. Soc.* **1982**, *104*, 7325.

(20) Nieuwenhuis, H. A.; van Loon, A.; Moraal, M. A.; Stufkens, D. J.; Oskam, A.; Goubitz, K. *Inorg. Chim. Acta* **1995**, *232*, 19.

(21) MeKolel-Veetil, M. K.; Rheingold, A. L.; Ahmed, K. J. *Organometallics* **1993**, *12*, 3439.

(22) Rosendorfer, P.; Mihan, S.; Niemer, B.; Beck, W. *Z. Naturforsch., B* **1995**, *50*, 1759.

[PF₆],²³ [Ir₃(μ-PPh₂)₃(CO)₄(^tBuNC)₃(Me)]I,²⁴ and [PPN]-[Ru₆(CO)₁₆(Me)].²⁵ In contrast there are numerous examples of dinuclear platinum A-frame complexes with one or more alkyl groups attached to the metal. No cluster compounds of first-row transition metals which also incorporate heavy main group atoms containing terminal alkyl groups have been reported to date. When main group-transition metal carbonylates are treated with alkylating agents, initial reaction may occur at (1) a main group metal atom, (2) one of the transition metals, or (3) one of the carbonyl ligands. It might be expected that reaction will occur at the main group atom when it retains a lone pair of electrons, but as shown for [Et₄N][BiFe₃(CO)₉(μ₃-CO)] the μ₃-bridging carbonyl oxygen is more basic and alkylation occurs there to give [BiFe₃(CO)₉(μ₃-CO)] upon treatment with methyl triflate.²⁶ Reaction of [E{Fe(CO)₄}₄]³⁻ (E = Sb, Bi) with RX, on the other hand, leads to products containing alkylated main group atoms.²⁷⁻²⁹ Herein we describe the first mixed main group transition-metal carbonyl clusters with a terminal alkyl ligand bound to the transition metal.

Experimental Section

General Methods. Unless otherwise specified, all synthetic manipulations were performed on a Schlenk line or in a drybox under an atmosphere of purified nitrogen using standard inert atmosphere techniques.³⁰ All solvents were distilled under nitrogen from the appropriate drying agents.^{31,32} Solution infrared spectra were obtained in 0.1 mm CaF₂ cells by using a Perkin-Elmer 1640 Fourier transform infrared spectrometer. ¹H and ¹³C spectra were recorded on a Bruker AC-250 spectrometer, operating at 250 MHz for ¹H and 62.9 MHz for ¹³C. ⁷⁷Se and ¹²⁵Te NMR spectra were recorded on an IBM/Bruker AF 300 spectrometer operating at 57.2 MHz (⁷⁷Se) and 94.8 MHz (¹²⁵Te). ⁷⁷Se and ¹²⁵Te NMR spectra were obtained using a 5 mm insert in a 10 mm NMR tube with the NMR solvent of choice, with neat Me₂Se or Me₂Te as reference (δ = 0). Coupling to protons was confirmed by running the experiment coupled and decoupled. Coupling constants were measured by ¹H NMR. ESI mass spectra were obtained on a Finnigan MAT 90 in MeOH in the negative ion mode. EI mass spectroscopy was performed on a Finnigan 3300 spectrometer. Elemental analysis (C, H, N) was performed in house using the Carlo Erba Instruments NA 1500 series 2 analyzer. EDAX (energy dispersive analytical X-ray spectroscopy, also known as EDS) analysis was obtained using a Cameca SX-50 microprobe with a SUN-based control and data reduction system. The compounds [PPN]₂[EFe₃(CO)₉] (E = S, [PPN]₂[Ib]);³³ E = Se, [PPN]₂[Ic]; E = Te, [PPN]₂[Id]), [PPN][HF₃(CO)₉E] (E

= Se, [PPN][Iic]; E = Te, [PPN][Iid]), [H₂Fe₃(CO)₉E] (E = Se, [Iic]; E = Te, [Iid]),¹⁵ [PPN]₂[Te{Fe(CO)₄}₃] [PPN]₂[Vid]),⁷ and [PPN]₂(μ-CuCl)Fe₃(CO)₉Te] ([PPN]₂[VIid])¹⁵ were prepared by the literature methods. [PPN][HF₃(CO)₉S] ([PPN]-[Iib]) and [H₂Fe₃(CO)₉S] ([IIIb]) were prepared analogously to their Se and Te counterparts. All compounds [Et₄N]₂[I] were prepared analogously to their PPN⁺ analogues. The spectroscopic properties of the [Et₄N]⁺ salts prepared this way closely match those for the [PPN]⁺ derivatives. Methyl triflate was carefully distilled and stored under inert atmosphere. Methyl iodide (MeI) was degassed by three successive freeze-pump-thaw-degas cycles and distilled bulb-to-bulb on the vacuum line from copper turnings.

Synthesis of [Et₄N][II]. A 10 mmol sample of the appropriate cluster [Et₄N]₂[I] was weighed into a 200 mL Schlenk flask in the drybox. A 100 mL portion of CH₂Cl₂ was added, and the suspension was stirred for 15 min. *p*-Toluenesulfonic acid (1.9 g, 10 mmol) was added in one portion, and the suspension was stirred until the solution became clear (about 0.5 h). Completeness of conversion was monitored by IR spectroscopy. The solvent was then removed in vacuo, and the residue was taken up in 30 mL of THF. An insoluble white powder, presumably [Et₄N][OTos], was filtered off, and the flask was placed in the freezer to complete precipitation of the [Et₄N][OTos]. The rest of the white powder was removed by filtration, and the solvent was removed in vacuo. The residue was redissolved in a minimal amount of MeOH (20 mL), and pure [Et₄N][II] was obtained as big chunks upon crystallizing at -20 °C. Yields were typically ca. 50%. The spectroscopic properties of this series of compounds match those previously obtained by a different route.^{13,34}

Synthesis of [PPN][Fe₃(CO)₉(SMe)]·Et₂O, [PPN][IVb]. To a 100 mL Schlenk flask charged with 1.50 g (1.0 mmol) of [PPN]₂[Ia] of was added 30 mL of CH₂Cl₂ followed by the addition of 0.11 mL (1.0 mmol) of methyl triflate via syringe. The solution was stirred overnight. The solvent was removed in vacuo, and ca. 60 mL of ether was added to the residue. The suspension was stirred for several hours in order to achieve complete dissolution of the product. An insoluble white powder was removed by filtration, and the solution was concentrated to ca. 15 mL and stored at -20 °C for several days. The product was isolated (0.55 g, 0.55 mmol; 55%) as red crystalline blocks. IR (ν_{CO}, cm⁻¹, CH₂Cl₂): 2033, 1970, 1944, 1917. NMR (δ, ppm, MeCN-*d*₃)¹H: 7.70–7.44 (PPN)⁺; 3.40 (MeS). ¹³C: 218.87 (CO), 134.95–130.58 (PPN)⁺, 26.67 (MeS). ESI: 446 (M⁻). Elemental anal. % calc (% found): C, 55.64 (55.49); H, 4.02 (3.83); N, 1.30 (1.38).

Synthesis of [PPN][MeFe₃(CO)₉Se], [PPN][Vc]. The reaction was performed similarly to the sulfur analogue using 1.66 g (1 mmol) of [PPN]₂[Ic] and 0.11 mL of methyl triflate in 30 mL of CH₂Cl₂. In addition, excess MeI can also be used if the reaction is performed in THF. Yield: 0.50 g (0.53 mmol; 53%). IR (ν_{CO}, cm⁻¹, CH₂Cl₂): 2043, 1989, 1977, 1839. NMR (δ, ppm, MeCN-*d*₃)¹H: 7.70–7.40 (PPN)⁺, 2.69 (MeFe). ¹³C: 244.80 (μ-CO), 217.93 (CO), 134.98–127.71 (PPN)⁺, 58.85 (MeFe). ⁷⁷Se: 662. The compound was enriched in ¹³CO by stirring a diluted solution of [PPN][Vc] in THF under 1 atm of ¹³CO (90% ¹³C; 10% ¹⁸O Cambridge Isotope Labs). NMR ¹³C (carbonyls only): (THF-*d*₈): 241.26 (μ-CO), 224.35, 220.38, 218.24 217.63 (CO). ESI: 514 (M⁻). Elemental anal. % calc (% found): C, 52.51 (52.35); H, 3.16 (3.65); N, 1.33 (1.43).

Synthesis of [PPN][MeFe₃(CO)₉Te], [PPN][Vd]. As per the Se analogue, in 20% yield. IR (ν_{CO}, cm⁻¹, MeCN): 2041, 2003, 1965, 1927, 1900; NMR (δ, ppm, MeCN-*d*₃)¹H: 7.65–7.47 (PPN)⁺, 2.51 (MeFe). ¹³C: 217 (CO); 133–127 (PPN)⁺; 50 (MeFe). ¹²⁵Te 1009. ESI: 562 (M⁻). Elemental anal. % calc (% found): C, 50.19 (49.60), H, 2.94 (3.02), N, 1.27 (1.35).

Low-Temperature NMR Studies. A 0.2 M solution of triflic acid in CD₂Cl₂ was prepared in the glovebox as well as

(23) Dawkins, G. M.; Green, M.; Orpen, A. G.; Stone, F. G. *J. Chem. Soc., Chem. Commun.* **1982**, 41.

(24) Shieh, M.; Browning, J.; Dixon, K. R.; Meanwell, N. J. *Organometallics* **1994**, *13*, 760.

(25) Chihara, T.; Aoki, K.; Yamazaki, H. *J. Organomet. Chem.* **1990**, *383*, 367.

(26) Whitmire, K. H.; Lagrone, C. B.; Rheingold, A. L. *Inorg. Chem.* **1986**, *25*, 2572.

(27) Shieh, M.; Liou, Y.; Peng, S.-M.; Lee, G.-H. *Inorg. Chem.* **1993**, *32*, 2212.

(28) Shieh, M.; Liou, Y.; B.-W., J. *Organometallics* **1993**, *12*, 4296.

(29) Shieh, M.; Sheu, C.-m.; Ho, L.-F.; Cherng, J.-J.; Jang, L. F.; Ueng, C.-H.; Peng, S.-M.; Lee, G. H. *Inorg. Chem.* **1996**, *35*, 5504.

(30) Shriver, D. F.; Drezdon, M. A. *The Manipulation of Air-Sensitive Compounds*; Wiley: New York, 1986.

(31) Gordon, A. J.; Ford, R. A. *The Chemist's Companion*; John Wiley and Sons: New York, 1972.

(32) Pangborn, A. B.; Giardello, M. A.; Grubbs, R. H.; Rosen, R. K.; Timmers, F. J. *Organometallics* **1996**, *15*, 1518.

(33) Holliday, R. L.; Roof, L. C.; Hargis, B.; Smith, D. M.; P. T., W.; Pennington, W. T.; Kolis, J. W. *Inorg. Chem.* **1995**, *34*, 4392.

(34) Shieh, M.; Tang, T.-F.; Peng, S.-M.; Lee, G.-H. *Inorg. Chem.* **1995**, *34*, 2797.

Table 1. Crystal Data^a

	[PPN] ₂ [Ib]· 0.7CH ₂ Cl ₂	[PPN][IIb]	IIIb
empirical formula	C _{81.70} H _{61.40} Cl _{1.40} · Fe ₃ N ₂ O ₉ P ₄ S	C ₄₅ H ₃₁ Fe ₃ · NO ₉ P ₂ S	C ₉ H ₂ Fe ₃ O ₉ S
fw	1588.25	991.26	453.72
cryst syst	monoclinic	monoclinic	monoclinic
space group	Cc (No. 9)	P2 ₁ /c (No. 14)	P2 ₁ /n (No. 14)
a, Å	29.279(20)	9.355(2)	8.937(2)
b, Å	14.675(8)	29.641(6)	14.736(3)
c, Å	21.463(15)	15.999(3)	11.434(2)
α, deg			
β, deg	123.82(4)	100.84(3)	103.64(3)
γ, deg			
volume, Å ³	7661.3(86)	4357.2(15)	1463.3(5)
Z	4	4	4
GOF (<i>F</i> ²)	1.032	1.025	1.043
R1 [<i>I</i> > 2σ(<i>I</i>)]	0.0514	0.0386	0.0284
wR2 [<i>I</i> > 2σ(<i>I</i>)]	0.1300	0.0858	0.0693
color	red	red	red
	[PPN][IVb]·Et ₂ O	[PPN][Vc]	
empirical formula	C ₅₀ H ₄₃ Fe ₃ NO ₁₀ P ₂ S	C ₄₆ H ₃₃ Fe ₃ NO ₉ P ₂ Se	
fw	1079.40	1052.18	
cryst syst	primitive	primitive	
space group	P $\bar{1}$ (No. 2)	P $\bar{1}$ (No. 2)	
a, Å	10.787(2)	11.818(2)	
b, Å	15.246(3)	13.312(3)	
c, Å	16.112(3)	14.893(3)	
α, deg	76.09(3)	82.98(3)	
β, deg	79.11(3)	84.48(3)	
γ, deg	89.82(3)	78.34(3)	
volume, Å ³	2523.2(8)	2271.3(8)	
Z	2	2	
GOF (<i>F</i> ²)	1.041	1.042	
R1 [<i>I</i> > 2σ(<i>I</i>)]	0.0512	0.0484	
wR2 [<i>I</i> > 2σ(<i>I</i>)]	0.0931	0.1008	
color	red	black	

^a R1 = $\sum |F_o| - |F_c| / \sum |F_o|$, wR2 = $[\sum w(F_o^2 - F_c^2)^2] / \sum [w(F_o^2)]^{1/2}$; $w = [\sigma^2(F_o^2) + (aP)^2 + bP]^{-1}$, where $P = (F_o^2 + 2F_c^2)/3$.

solutions of 0.1 mmol of the cluster in 0.5 mL of CD₂Cl₂. Both solutions were cooled to -78 °C in a dry ice/acetone bath, and 0.5 mL of the acid solution was quickly transferred to the solution containing the cluster. The tube was then immediately frozen in liquid N₂ and sealed under vacuum for storage. Just before measurement, the tube was warmed to -78 °C and transferred to the precooled NMR probe. ¹³C VT studies were performed in THF-*d*₈ from 180 K to room temperature on an enriched sample of [PPN][Vc].

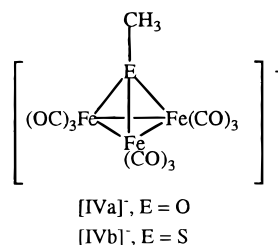
X-ray Crystallography. Single Crystals of [PPN]₂[Ib] were grown from CH₂Cl₂/Et₂O, while those of [PPN][IIb] were grown by slow diffusion of diisopropyl ether into a concentrated THF solution at -20 °C. Single crystals of [IIIb], [PPN][IVb] and [PPN][Vc] were grown from Et₂O at -20 °C. All crystals selected for data collection were mounted on the tip of a glass fiber with epoxy resin. Data were collected at -50 °C on a Rigaku AFC5-S automated four-circle diffractometer using the TEXSAN 5.0 software package³⁵ and were corrected for Lorentz/polarization effects. The data of [PPN]₂[Ib], [IIIb], and [PPN][Vc] were corrected for absorption using Ψ -scans. Data collection and refinement parameters are summarized in Table 1. Scattering factors were taken from the literature.³⁶ Structures were solved using the SHELXTL-PLUS package on a PC.³⁷ Refinements on *F*² using all reflections except those with very negative *F*² were performed with SHELXL-93 on a PC or a SUN workstation running SOLARIS.³⁸ Weighted

R-factors (*wR*) and all goodnesses of fit (*S*) are based on *F*²; conventional *R*-factors (*R*) are based on *F*, with *F* set to zero for negative *F*². *R*-factors based on *F*² are statistically about twice as large as those based on *F*. The weighting factor $w = [\sigma^2(F_o^2) + (aP)^2 + bP]^{-1}$, where $P = (F_o^2 + 2F_c^2)/3$, was refined for *a* and *b*. Hydrogen atoms were included in their calculated positions, except for the hydride atoms of [PPN][IIb] and [IIIb], which were found in the difference Fourier map. The choice of absolute structure of [PPN]₂[Ib] was based upon the refinement of the Flack parameter.³⁹

Results and Discussion

Syntheses. There are two likely sites where alkylation reactions can occur for [EFe₃(CO)₉]²⁻ clusters which contain only terminal carbonyl ligands: the lone pair on the chalcogenide atom and the Fe₃ base. Fenske Hall calculations on [Ia]²⁻ and [Ib]²⁻ have shown that both compounds have very similar orbital structures¹⁶ and suggest that the Fe₃(CO)₉ fragment can readily adjust itself to the size of the chalcogenide by minor changes in the overall bonding. Since the transition metal component remains the same for the series examined, the differences in reactivity will largely depend on the basicity/diffuseness of the lone pair of electrons on E.

The reaction of [Ib]²⁻ with methyl triflate occurs at the sulfur atom, similarly to the reported alkylation of [Ia]²⁻.⁴⁰ The structural parameters of [PPN][IVb] are comparable to the ^tBu analogue, [(^tPr)₂NH₂][Fe₃(CO)₉-(S^tBu)], which was obtained through direct reaction of ^tBuSH and Fe₃(CO)₁₂ followed by treatment with base.^{41,42} The Fe-S and Fe-Fe bond distances in the parent [Ib]²⁻ and [IVb]⁻ are similar.



Protonation contrasts with alkylation in that it always occurs at the Fe₃ base.¹⁶ The Fe₃(CO)₉ fragment is quite basic. The p*K*_a, for instance, of HFe₃(CO)₉Scy (cy = cyclohexyl) in MeCN is 16.⁴³ Reactions of [I]²⁻ with both protic and Lewis acids such as Hg²⁺, (Ph₃P)Au⁺, or Cu⁺ all occur on the Fe₃ unit rather than the chalcogenide.⁹⁻¹⁵ On the other hand, the reaction between [Ib]²⁻ and Re-(CO)₅(O₃SCF₃) yields the stable [Fe₃(CO)₉(SRe(CO)₅)]⁻,¹⁶ probably as a result of steric inhibition of the access to the iron centers.

Because of this difference in reactivity of [Ib]²⁻ toward Me⁺ and H⁺, the protonation of [Ib]²⁻ was followed at -78 °C by NMR, to determine if initial attack of the cluster might actually occur at the S followed by a migration to the Fe₃ framework. Such a transfer occurs

(39) Flack, H. D. *Acta Crystallogr.* **1983**, A39, 876.

(40) Ceriotti, A.; Resconi, L.; Demartin, F.; Longoni, G.; Manassero, M.; Sansoni, M. *J. Organomet. Chem.* **1983**, 249, C35.

(41) Winter, A.; Zsolnai, L.; Huttner, G. *Chem. Ber.* **1982**, 115, 1286.

(42) Winter, A.; Zsolnai, L.; Huttner, G. *J. Organomet. Chem.* **1983**, 250, 409.

(43) Kristjánsdóttin, S. S.; Moody, A. E.; Weberg, R. T.; Norton, J. R. *Organometallics* **1988**, 7, 1983.

(35) TEXSAN: Single-Crystal Structure Analysis Software 5.0; Molecular Structure Co.: The Woodlands, TX, 1990.

(36) International Tables for Crystallography; Kluwers Academic Publishers: Dordrecht, 1992; Vol. C; Tables 4.2.6.8, and 6.1.1.4.

(37) Sheldrick, G. M. *SHELXTL PLUS PC 5.0*; Siemens Crystallographic Research Systems: Madison, WI, 1995.

(38) Sheldrick, G. M. *SHELXL-93*, Göttingen, Germany, 1993.

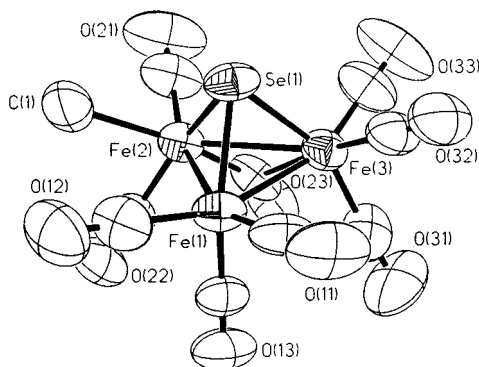
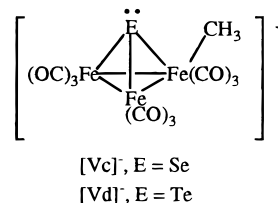


Figure 1. Thermal ellipsoid plot (50% probability) of the cluster anion of [PPN][Vc].

in the case of $[\text{HFe}_3(\text{CO})_{11}]^-$.^{44–46} For $[\text{Ru}_3(\text{CO})_{10}(\text{NO})]^-$ protonation occurred at the oxygen atom of the NO ligand at low temperatures, but the proton migrated to the metal framework upon heating the sample to room temperature.⁴⁷ However, for the low-temperature protonation of $[\text{Ib}]^{2-}$ only signals attributable to residual solvent and the iron hydride were observed. A similar phenomenon had been observed for the heavier chalcogenides where only signals attributable to the iron hydride were observed upon low-temperature protonation. This supports the previous view that the electrophilic attack takes place directly at the Fe–Fe bond.¹⁵

In marked contrast $[\text{Ic}]^-$ clearly shows the methyl group has attached itself to the iron atom giving [PPN][Vc] (Figure 1). The structure consists of two seven-coordinate iron atoms and one conventional six-coordinate iron center. This manifests itself in the longer Fe–Fe bond (2.697(2) Å) between the two seven-coordinate iron atoms, making the cluster quite asymmetric. The Fe–Me bond distance (2.226(9) Å) is considerably longer than other Fe–Me single bonds known in neutral and cationic compounds such as $\text{Fe}(\text{C}_{10}\text{H}_{19}\text{N}_8)(\text{CO})(\text{Me})$ ⁴⁸ (2.077 Å), $[\text{Fe}_2(\mu\text{-Me})_2(\mu\text{-CO})(\mu\text{-dppm})(\text{Cp})_2]^+$ ¹⁹ (2.008 and 2.108 Å), phthalocyanines (2.025 Å),⁴⁹ or an Fe(III) porphyrin (1.979 Å),⁵⁰ and even longer than the Fe–C_{alkyl} bond distances in $[\text{PPN}][\text{RFe}(\text{CO})_4]$ (R = C₃H₇, 2.20(2) Å,⁵¹ CH₂COOMe, 2.151(6) Å,⁵² CH–(Me)(COOEt), 2.164(3) Å).⁵³ Consistent with this longer bond length, the ¹H shift for the methyl group is about 2.5 ppm more downfield than in the neutral and cationic compounds, for which the proton signal generally appears around 0 ppm, and about 0.2 ppm more downfield than the shift in $[\text{PPN}][(\text{CO})_4\text{Fe}\{\text{CH}(\text{Me})(\text{COOEt})\}]$.⁵⁴ This indicates a very weak bond, consistent with the observed reactivity. Protonation at room temperature (RT) of $[\text{Vc}]^-$ yielded the monohydride $[\text{Iic}]^-$ and at –78

°C an intractable paramagnetic mixture. Reaction with CO (500 psi, RT) yielded $\text{Fe}(\text{CO})_5$ as the main product. It is interesting that the alkylated product is much more susceptible to fragmentation than the parent dianion or the monohydride (*vide infra*).



An enriched sample of $[\text{Vc}]^-$, obtained by exchange with ¹³CO, shows five peaks assignable to carbonyl ligands. This indicates that the solid-state structure is basically retained in solution. According to the symmetry of $[\text{Vc}]^-$, all nine carbonyl ligands should be unique. Scrambling processes, however, can cause the averaging of some signals, or some signals could be “accidentally degenerate” or not resolvable under the conditions of the experiment. In the room-temperature spectrum, the signal for the bridging carbonyl can easily be assigned at 241.26 ppm. A VT ¹³C study was performed to help resolve these issues, but even though the spectrum changed with new signals present at low temperature, the spectrum did not completely resolve even at 180 K, the low-temperature limit of our instrument. It is noteworthy, however, that the CO fluxionality has been greatly restricted by the presence of the E and Me functions since the other iron carbonyl clusters show complete scrambling of all the CO ligands at room temperature and, in some cases, even to –150 °C. The reaction of $[\text{Id}]^{2-}$ with methyl triflate also yielded alkylation at the Fe₃ base, a conclusion based on nearly identical spectroscopic properties compared to the Se analogue.

The difference in the reactivity in the series $[\text{I}]^{2-}$ toward alkylating agents can be rationalized on the basis of the different nucleophilicities of the chalcogen atom, which in this case are directly related to the atomic bond radii.³⁷ The largest difference in bond radius occurs between two elements O and S (1.160 and 1.530 Å, a 32% increase with respect to O). The difference between S and the heavier chalcogens is considerably smaller (Se = 1.670, a 9% increase with respect to S, Te = 1.879 Å, a 12.5% increase with respect to Se). As mentioned above, the Fe₃(CO)₉ fragment can accommodate all chalcogenides by minor adjustments in the overall bonding scheme. For reasons of comparison, the crystal structures of $[\text{PPN}]_2[\text{Ib}]$, $[\text{PPN}][\text{IIb}]$, and $[\text{IIIb}]$ were obtained. Since these structures are not unusual, a full presentation is confined to the Supporting Information, with the notable bond distances given in Table 4. Throughout this series the E–Fe distances remain constant for each three-coordinated E (average values: 1.892(3) Å for O, 2.200(6) Å for S, 2.321(1) Å for Se, and 2.494(6) Å for Te). The increase in E–M distances follows the trend of the increase in the bond radius of the respective elements ($d_{\text{Fe-S}} = 1.16d_{\text{Fe-O}}$; $d_{\text{Fe-Se}} = 1.055d_{\text{Fe-S}}$; $d_{\text{Fe-Te}} = 1.073d_{\text{Fe-Se}}$). Upon protonation, the H-bridged Fe–Fe distances increase significantly, as is well-precedented in the literature.⁵⁴

(44) Hodali, H. A.; Shriver, D. F.; Ammlung, C. A. *J. Am. Chem. Soc.* **1978**, *100*, 5239.

(45) Kiester, J. B. *J. Organomet. Chem.* **1980**, *190*, C36.

(46) Fachinetti, G. *J. Chem. Soc., Chem. Commun.* **1979**.

(47) Gladfelter, W. L. *Adv. Organomet. Chem.* **1985**, *24*, 41.

(48) Goedken, V.; Peng, S.-M. *J. Am. Chem. Soc.* **1974**, *96*, 7826.

(49) Tahiri, M.; Doppelt, P.; Fischer, J.; Wiess, R. *Inorg. Chem.* **1988**, *27*, 2897.

(50) Balch, A. L.; Olmstead, M. M.; Safari, N.; St. Claire, T. M. *Inorg. Chem.* **1994**, *33*, 2815.

(51) Huttner, G.; Gartzke, W. *Chem. Ber.* **1975**, *108*, 1373.

(52) Keim, W.; Röper, M.; Strutz, H.; Krüger, C. *Angew. Chem., Int. Ed. Engl.* **1984**, *23*, 432.

(53) Brunet, J.-J.; Dahan, F.; Passelaigue, E. *Acta Crystallogr.* **1992**, *C48*, 1103.

(54) Brunet, J.-J.; Passelaigue, E. *J. Organomet. Chem.* **1989**, *375*, 203.

Table 2. Selected Bond Distances and Angles for [PPN][Vc]

Se(1)–Fe(1)	2.2539(14)	Se(1)–Fe(2)	2.3125(13)
Se(1)–Fe(3)	2.3439(14)	Fe(1)–Fe(2)	2.548(2)
Fe(1)–Fe(3)	2.589(2)	Fe(2)–Fe(3)	2.697(2)
Fe(2)–C(1)	2.226(9)		
Se(1)–Fe(1)–Fe(2)	57.19(4)	Se(1)–Fe(1)–Fe(3)	57.39(4)
Se(1)–Fe(2)–Fe(1)	55.00(4)	Se(1)–Fe(2)–Fe(3)	55.16(4)
Se(1)–Fe(3)–Fe(1)	54.10(4)	Se(1)–Fe(3)–Fe(2)	54.07(4)
Fe(1)–Se(1)–Fe(2)	67.81(4)	Fe(1)–Se(1)–Fe(3)	68.52(4)
Fe(1)–Fe(2)–Fe(3)	59.09(4)	Fe(1)–Fe(3)–Fe(2)	57.59(4)
Fe(2)–Se(1)–Fe(3)	70.77(4)	Fe(2)–Fe(1)–Fe(3)	63.32(5)
C(1)–Fe(2)–Se(1)	88.3(3)	C(1)–Fe(2)–Fe(1)	96.2(2)

Table 3. ^{77}Se and ^{125}Te NMR Shifts (ppm) of Se and Te Cluster Compounds

	E = Se	E = Te
[I] $^{2-}$	539	399
[II] $^-$	587(d)	529
[III]	669(t)	744
[V] $^-$	662(m)	1090
[VI] $^{2-}$		556
[VII] $^{2-}$		352

Since the bonding between the chalcogen atom and the Fe_3 triangle is quite similar, the O atom of the [Ia] $^{2-}$ is expected to be the most nucleophilic of the series. This is indeed observed. Both protonation and alkylation take place at the O atom.⁴⁰ The orbitals for the S atom are more spatially diffuse; therefore, the reaction of [Ib] $^{2-}$ with Lewis or protic acids, or Me^+ , could occur at either the S atom or the Fe_3 base. However, only for Me^+ is reaction at the S observed, and this may be directed by steric crowding at the metal centers. All other reactions take place at the Fe_3 base. For [Ic] $^{2-}$ and [Id] $^{2-}$, the orbitals around the Se and Te atom have become so spatially diffuse that even the reaction with Me^+ occurs at the Fe_3 base, despite steric crowding that may occur here.

As noted before for the IR and ^{13}C data of the series of clusters [I] $^{2-}$ –[III], the removal of electron density on the cluster can be seen spectroscopically from trends in the shifts of the ^{13}C and IR ν_{CO} signals.¹⁵ The ^{13}C signals for the CO's and IR CO stretching frequencies for [IVb] $^-$, [Vc] $^-$, and [Vd] $^-$ are similar to those reported for [II] and [III] $^-$. The downfield the shifts of the ^{77}Se and ^{125}Te signals (Table 3) upon protonation or alkylation support this view of decreased electron

(55) Whitmire, K. H. Iron Compounds without hydrocarbon ligands. In *Comprehensive Organometallic Chemistry II*; Shriver, D. F., Bruce, M. I., Eds.; Aken, W. W., Stone, F. G. A., Wilkinson, G., Eds. in Chief; Pergamon Press Publishers: New York, 1995; Vol. 7, pp 1–99.

Table 4. Comparison of Fe–Fe and E–Fe Bond Distances (E = O, S, Se, Te)

	Fe–Fe	Fe– μX –Fe ([II] $^-$ and III, X = H; [VII] $^{2-}$, X = CuCl)	E–Fe	ref
[Ia] $^{2-}$	2.484(7)*		1.892(3)*	38
[Ib] $^{2-}$	2.596(9)*		2.201(6)*	a
[Ic] $^{2-}$	2.61(1)*		2.322(9)*	7
[Id] $^{2-}$	2.631(7)*		2.490(2)*	7
[IIb] $^-$	2.5836(6)*	2.6534(10)	2.20(2)*	a
[IIc] $^-$	2.615(8)*	2.689(3)	2.32(2)*	15
[IId] $^-$	2.63(1)*	2.7276(10)	2.491(3)*	15
[IIe] $^-$	2.739(3)*	2.871(2)	2.36(2)*	a
[IIIb]	2.6006(8)	2.65(2)*	2.20(2)*	a
[IIIc]	2.6065(8)	2.686(6)*	2.32(4)*	15
[IIId]	2.6741(9)	2.70(3)*	2.50(1)*	15
[IIIe]	2.760(1)	2.881(2)*	2.36(1)*	63
[IVb] $^-$	2.636(3)*		2.130(5)*	a
[VI] $^{2-}$			2.490(2)*	7
[VII] $^{2-}$	2.65(1)*	2.738(3)	2.490(4)*	15

^a This work. * denotes average values where error is calculated using the scatter formula

$$\sigma = \left[\sum_{i=1}^N (d_i - d)^2 / (N - 1) \right]^{1/2}$$

density on the cluster. The shift upon the second protonation is about twice as large as the shift for the first protonation step. In contrast, the addition of CuCl to the Te cluster¹⁵ shows a upfield shift, which suggests increased electron density to the cluster. The upfield shift upon the formation of [Id] $^{2-}$ from the open cluster [VI] $^{2-}$ is also indicative of the increased electron density being shifted toward the main group element upon closing.

Acknowledgment. This work was assisted by a grant from the Robert A. Welch foundation and the National Science Foundation (Grant CHE-9408613). We also wish to thank Dr. Lawrence B. Alemany for his assistance in obtaining the ^{77}Se and ^{125}Te spectra and Dr. Terry D. Marriott for collecting mass spectrometric data.

Supporting Information Available: A listing of complete crystallographic data for [PPN] $_2$ [Ib], [PPN][IIb], [IIIb], [PPN]-[IVb], and [PPN][Vc] (41 pages). This material is contained in many libraries on microfiche, immediately follows this article in the microfilm version of the journal, can be ordered from the ACS, and can be downloaded from the Internet; see any current masthead page for ordering information and Internet access instructions.

OM980428V